Check for
updates

Amine modified nanozeolites for the three component synthesis of chromenes

**Fatemeh Babaei[1] · Sakineh Asghari[1,2] · Mahmoud Tajbakhsh[1]**

Abstract

New amine modified nanozeolites were prepared and characterized using FT-IR, TGA, DTG, SEM, and TEM. Then the synthesized nanozeolites were employed as novel, recyclable and safe catalysts for the one-pot, three-component condensation of 4-hydroxycoumarin with aldehydes and malononitrile to produce new and known pyrano[2,3-*c*]chromenes as potent biologically active compounds. This novel method has many advantages, such as high product yield and a simple work-up procedure.

Graphical abstract
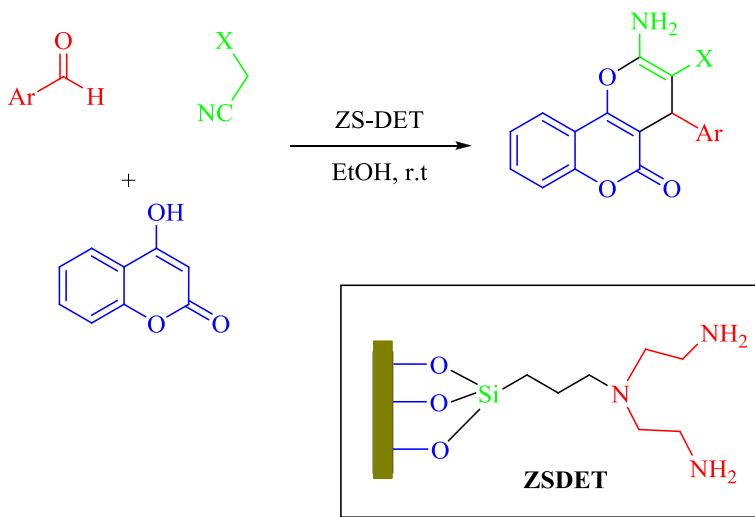
Extended author information available on the last page of the article
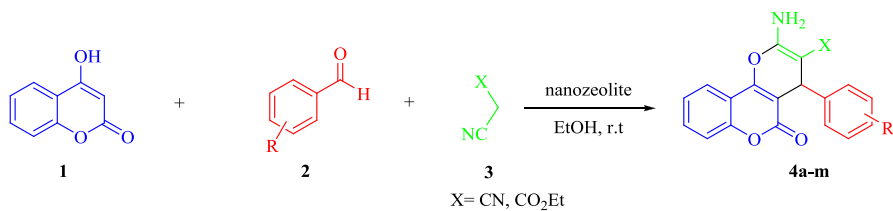
Scheme 1 Synthesis of 3,4-dihydropyrano[*c*] chromenes using amine functionalized nanozeolites

Introduction

Multicomponent reactions (MCRs) are special types of synthetically useful organic reactions in which three or more various substrates react to give a final product in a one-pot procedure [1, 2]. These reactions are a powerful tool in the organic synthesis and pharmaceutical chemistry, due to their wide range of usage in the preparation of various structural scaffolds and discovery of new drugs [3–5]. The 3,4-Dihydropyrano[c] chromene and its derivatives are very useful compounds in various fields of chemistry, biology and pharmacology. Some of these compounds exist widely in natural products and exhibit many features such as anticancer, anti-anaphylactin, anticoagulant, diuretic, and spasmolytic activities [6–9]. In addition, they have been applied to cure neurodegenerative disorders, such as Alzheimer's disease, amyotrophic lateral sclerosis, Parkinson's disease, Huntington's disease and Down's syndrome for the treatment of schizophrenia and myoclonus [10].

These compounds have been prepared from reaction of aromatic aldehyde, malononitrile and 4-hydroxycoumarin in the presence of a variety of acidic catalysts including diammonium hydrogen phosphate (DAHP) [11], $H_6P_2W_{18}O_{62} \cdot 18H_2O$ [12] and various bases like pyridine [13], tetrabutylammonium bromide (TBAB) [14] and (*S*)-proline [11]. However, many of these reported methods suffer from drawbacks like harsh reaction conditions, low yields, time-consuming reaction, cumbersome product isolation procedures and difficulty in recovery and reusability of the catalysts. Therefore, the progress of novel approaches for synthesizing these compounds is a great goal for organic chemists and pharmacists.

The use of heterogeneous catalysts in organic synthesis is a fascinating method to access green catalysts, because they are well-matched with high-interest in different processes of environmentally friendly chemical transformations [15]. Recently, the preparation of catalysts based on zeolites and associated compounds has attracted high attention in synthetic chemistry and technology, due to some reasons such as the lack of need for separation through distillation or extraction [16–18]. Nanozeolites have unique properties including excellent thermal stability, easy availability, nontoxicity, low cost and reusability [19–21]. Because of extremely small dimensions and large surface-to-volume ratio of nanozeolites, which increase the rate and the reaction selectivity, we report here the synthesis of new modified nanozeolites with multifunctional amines, and use them in the three component reaction of 4-hydroxycoumarin **1**, aromatic aldehyde **2** and malononitrile for synthesizing 3,4-dihydropyrano[c] chromenes (Scheme 1).

Experimental

Methods and materials

The chemicals such as (3-chloropropyl trimethoxysilane) (CPTMS), diethylenetriamine (DET), triethylenetetramine (TET) and tetraethylenepentamine (TEP) were purchased from Merk (Germany). All the solvents were obtained from Sigma-Aldrich Chemical Co. (St Louis, MO, USA). NaY nanozeolite with Si/Al = 2.5 was purchased from Zeolyst company (USA). Fourier transform infrared (FT-IR) spectra of the neat and functionalized nanozeolites were taken by means of a Bruker Tensor 27 spectrometer (Bruker, Karlsruhe, Germany). Vibration bands were reported as the wavenumber (cm^{-1}) and the spectra were recorded using the KBr method. Melting points were measured in open glass capillaries using an Electrothermal IA9100 series digital melting point apparatus (Electrothermal, Essex, UK). ^1H and ^{13}C NMR spectra were obtained in $CDCl_3$ solution by means of a Bruker Avance DRX-400 spectrometer (Bruker, Ettlingen, Germany) at a temperature of 25 °C. Thermo gravimetric analysis (TGA) was carried out on a Netzsch TG 209 F1 analyzer (Netzsch, Selb, Germany) from ambient temperature to 600 °C at a heating rate of 10 °C per min under a nitrogen atmosphere. The morphology and the chemical composition of the products were characterized using high-resolution field emission scanning electron microscopy on a MIRA 3-XMU (Tescan, Brno, Czech Republic) coupled with energy dispersive X-ray analysis (FE-SEM/EDX). The specific surface area, pore volume, and pore size distribution were measured by the nitrogen adsorption–desorption method using the Brunauer–Emmett–Teller (BET) model and t-plot. All data were recorded and analyzed with BELsorp, Japan.

General procedure for the synthesis of amine modified nanozeolites with multifunctional amines (ZS-DET, ZS-TET, ZS-TEP)

To a three-necked round-bottomed flask equipped with a magnetic stirrer, a nitrogen inlet and reflux condenser, NaY nanozeolite (1 g) was added into 30 mL of anhydrous toluene at 110 °C for 30 min. Then 1.82 mL (10 mmol) of (3-chloropropyl trimethoxysilane) (CPTMS) was poured into the mixture. The reaction mixture was refluxed for 4 h. Then, the mixture was cooled and filtrated to separate the solid residue. For removing of non-grafted CPTMS, the solid was placed in a Soxhlet extractor and extracted by 150 mL of ethanol (99.5%) for 24 h. Then, the obtained silane–functionalized zeolite (ZS) was poured into 30 mL of anhydrous dichloromethane at ambient temperature under an inert atmosphere of nitrogen. Then, 1.38 mL (10 mmol) of triethylamine and 10 mmol of the respective amine (DET, TET or TEP) were poured into the mixture and stirred for 24 h. The catalyst was isolated via filtration. To remove the non-grafted amine, the solid was placed in a Soxhlet extractor and extracted by 150 mL of ethanol (99.5%) for 24 h. The obtained solid was dried in an oven overnight.

General procedure to prepare pyrano[2,3-*c*]coumarin derivatives 4a-am

4-Hydroxycoumarin **1** (1 mmol), aromatic aldehydes **2** (1 mmol), malononitrile **3** (1.1 mmol) and ZS-DET (10 mg) were added to a 10 mL EtOH in a 25-mL Pyrex flask and stirred for an appropriate time (Table 3). Progress of the reaction was controlled by thin layer chromatography (TLC) using hexane/EtOAc (3:2). At the end of the reaction, nano-zeolit catalyst (ZS-DET) was separated through filtration. The solvent of the residue solution was removed under vacuum, and then the residue was recrystallized in EtOH to produce the compounds **4a–4m**.

Spectral data

Compound 4a ^{1}H NMR (DMSO, 400 MHz): δ 7.90 (dd, 1H, $J = 8.0$, 1.6 Hz), 7.72 (td, 1H, $J = 8.0$, 1.6 Hz), 7.50 (d, 2H, $J = 8.4$ Hz), 7.48–7.45 (m, 4H), 7.25 (d, 2H, $J = 8.4$ Hz), 4.47 (s, 1H). ^{13}C NMR (DMSO, 100 MHz): δ 160.00, 158.40, 158.36, 154.02, 152.64, 143.22, 133.49, 131.82, 130.48, 125.16, 122.97, 120.69, 119.56, 117.06, 113.40, 103.88, 57.87.

Compound 4b ^{1}H NMR (DMSO, 400 MHz): δ 7.90 (dd, 1H, $J = 8.0$, 1.6 Hz), 7.72 (td, 1H, $J = 8.0$, 1.6 Hz), 7.50 (t, 2H, $J = 7.2$ Hz), 7.45 (s, 2H), 7.37 (d, 2H, $J = 8.4$ Hz), 7.31 (d, 2H, $J = 8.4$ Hz), 4.49 (s, 1H). ^{13}C NMR (DMSO, 100 MHz): δ 160.00, 158.42, 158.38, 154.02, 152.65, 142.79, 133.48, 132.15, 130.11, 128.90, 125.16, 122.98, 119.54, 117.05, 113.41, 103.95, 57.97, 36.89, 36.85.

Compound 4c ^{1}H NMR (DMSO, 400 MHz): δ 7.91 (dd, 1H, $J = 8.0$, 1.6 Hz), 7.80 (d, 2H, $J = 8.4$ Hz), 7.73 (td, 1H, $J = 8.0$, 1.6 Hz), 7.51 (d, 2H, $J = 8.4$ Hz), 7.49–7.46 (m, 4H), 4.60 (s, 1H). ^{13}C NMR (DMSO, 100 MHz): δ 160.04, 158.49, 154.40, 152.72, 149.25, 133.60, 132.97, 129.36, 125.19, 123.04, 119.40, 119.19, 117.09, 113.40, 110.41, 103.33, 57.35, 37.47.

Compound 4d ^{1}H NMR (DMSO, 400 MHz): δ 7.91 (dd, 1H, $J = 8.0$, 1.6 Hz), 7.80 (d, 2H, $J = 8.4$ Hz), 7.73 (td, 1H, $J = 8.0$, 1.6 Hz), 7.51 (d, 2H, $J = 8.4$ Hz), 7.49–7.46 (m, 4H), 4.60 (s, 1H). ^{13}C NMR (DMSO, 100 MHz): δ 160.04, 158.49, 154.40, 152.72, 149.25, 133.60, 132.97, 129.36, 125.19, 123.04, 119.40, 119.19, 117.09, 113.40, 110.41, 103.33, 57.35, 37.47.

Compound 4e ^{1}H NMR (DMSO, 400 MHz): δ 7.92–7.89 (m, 2H), 7.72 (td, 1H, $J = 8.0$, 1.6 Hz), 7.66 (td, 1H, $J = 8.0$, 1.2 Hz), 7.56 (s, 2H), 7.54–7.53 (m, 1H), 7.52-7.51 (m, 1H), 7.50-7.47 (m, 1H), 7.45 (d, 1H, $J = 8.4$ Hz), 5.25 (s, 1H). ^{13}C NMR (DMSO, 100 MHz): δ 160.18, 159.06, 159.02, 154.06, 152.64, 149.64, 137.80, 134.15, 133.59, 131.62, 128.93, 125.24, 124.43, 123.03, 119.14, 117.12, 113.30, 103.77, 56.53, 32.06, 32.01.

Compound 4f ^{1}H NMR (DMSO, 400 MHz): δ 7.90 (dd, 1H, $J = 8.0$, 1.6 Hz), 7.73 (td, 1H, $J = 8.0$, 1.6 Hz), 7.58 (d, 1H, $J = 2.0$ Hz), 7.53–7.47 (m, 4H), 7.39 (d, 1H, $J = 8.4$ Hz), 7.35 (dd, 1H, $J = 8.4$, 2.0 Hz), 4.98 (s, 1H). ^{13}C NMR (DMSO, 100 MHz): δ 159.89, 158.59, 154.62, 152.69, 139.88, 133.60, 132.85, 132.56, 129.32, 128.34, 125.22, 123.00, 119.15, 117.10, 113.28, 102.94, 56.46, 34.38.

Compound 4h ^{1}H NMR (CDCL$_3$, 400 MHz): 8.06 (d, 1H, $J = 7.2$ Hz), 7.83 (dd, 1H, $J = 7.2$, 1.6 Hz), 7.57 (td, 1H, $J = 8.0$, 1.6 Hz), 7.35-7.30 (m, 3H), 7.17 (d, 1H, $J = 8.4$ Hz), 4.91 (s, 1H), 4.09 (q, 2H, $J = 7.2$ Hz), 1.19 (t, 3H, $J = 7.2$ Hz). ^{13}C NMR (CDCL$_3$, 100 MHz): δ 168.55, 160.67, 157.95, 152.84, 152.60, 142.90, 132.32, 131.09, 129.89, 128.24, 128.15, 125.21, 124.36, 123.36, 122.26, 116.89, 113.35, 107.42, 79.72, 35.07, 14.19.

Compound 4i ^{1}H NMR (CDCL$_3$, 400 MHz): 8.06 (d, 1H, $J = 7.2$ Hz), 7.83 (dd, 1H, $J = 7.2$, 1.6 Hz), 7.57 (td, 1H, $J = 8.0$, 1.6 Hz), 7.35–7.30 (m, 3H), 7.17 (d, 1H, $J = 8.4$ Hz), 4.91 (s, 1H), 4.09 (q, 2H, $J = 7.2$ Hz), 1.19 (t, 3H, $J = 7.2$ Hz). ^{13}C NMR (CDCL$_3$, 100 MHz): δ 168.55, 160.67, 157.95, 152.84, 152.60, 142.90, 132.32, 131.09, 129.89, 128.24, 128.15, 125.21, 124.36, 123.36, 122.26, 116.89, 113.35, 107.42, 79.72, 35.07, 14.19.

Compound 4j ^{1}H NMR (CDCL$_3$, 400 MHz): δ 7.84 (dd, 1H, $J = 8.0$ Hz), 7.58 (td, 1H, $J = 8.4$, 1.6 Hz), 7.36–7.32 (m, 3H), 7.29 (d, 1H, $J = 2.4$ Hz), 7.15 (dd, 1H, $J = 8.0$, 2.4 Hz), 6.57 (s, 2H), 5.21 (s, 2H), 4.09 (q, 2H, $J = 7.2$ Hz), 1.19 (t, 3H, $J = 7.2$ Hz). ^{13}C NMR (CDCL$_3$, 100 MHz): δ 168.60, 160.37, 158.11, 153.78, 152.72, 139.11, 134.65, 133.55, 132.95, 132.46, 129.63, 126.58, 124.35, 122.34, 116.91, 113.08, 105.25, 78.13, 60.13, 34.26, 14.22.

Compound 4k ^{1}H NMR (DMSO, 400 MHz): δ 7.98 (dd, 1H, $J = 8.0$, 1.6 Hz), 7.93 (s, 2H), 7.71 (d, 2H, $J = 8.0$ Hz), 7.69 (dd, 1H, $J = 8.0$, 1.6 Hz), 7.49 (td, 1H, $J = 8.0$, 1.2 Hz), 7.44 (d, 3H, $J = 8.0$ Hz), 4.74 (s, 1H), 3.98 (q, 2H, $J = 7.2$ Hz), 1.08 (t, 3H, $J = 7.2$ Hz). ^{13}C NMR (DMSO, 100 MHz): δ 167.74, 160.33, 158.97, 153.98, 152.65, 150.99, 133.40, 132.42, 129.77, 125.15, 123.07, 119.31, 117.03, 113.48, 109.65, 106.02, 76.46, 59.62, 36.21, 14.61, 14.58.

Compound 4l ^{1}H NMR (DMSO, 400 MHz): δ 8.12 (d, 2H, $J = 8.8$ Hz), 7.99 (dd, 1H, $J = 8.0$, 1.6 Hz), 7.96 (s, 2H), 7.71 (td, 1H, $J = 8.0$, 1.6 Hz), 7.53 (d, 2H, $J = 8.8$ Hz), 7.50–7.48 (m, 1H), 7.45 (d, 1H, $J = 8.4$ Hz), 4.81 (s, 1H), 3.98 (q, 2H, $J = 7.2$ Hz), 1.10 (t, 3H, $J = 7.2$ Hz). ^{13}C NMR (DMSO, 100 MHz): δ 167.70, 160.31, 158.96, 158.90, 154.02, 153.04, 152.70, 146.54, 133.45, 130.02, 125.17, 123.68, 123.08, 117.07, 113.48, 105.92, 76.34, 59.65, 36.06, 14.60.

Compound 4m ^{1}H NMR (DMSO, 400 MHz): δ 8.12 (d, 2H, $J = 8.8$ Hz), 7.99 (dd, 1H, $J = 8.0$, 1.6 Hz), 7.96 (s, 2H), 7.71 (td, 1H, $J = 8.0$, 1.6 Hz), 7.53 (d, 2H, $J = 8.8$ Hz), 7.50–7.48 (m, 1H), 7.45 (d, 1H, $J = 8.4$ Hz), 4.81 (s, 1H), 3.98 (q, 2H, $J = 7.2$ Hz), 1.10 (t, 3H, $J = 7.2$ Hz). ^{13}C NMR (DMSO, 100 MHz): δ 167.70, 160.31, 158.96, 158.90, 154.02, 153.04, 152.70, 146.54, 133.45, 130.02, 125.17, 123.68, 123.08, 117.07, 113.48, 105.92, 76.34, 59.65, 36.06, 14.60.

Results and discussion

Initially NaY nanozolite (Z) has been reacted with CPTMS leading silane–functionalized zeolite (ZS). Then, it was reacted with DET as a tridentate amine to afford ZS-DET as a basic nanocatalyst. Similarly, TET (as a tetradentate amine) and TEP (as a pentadentate amine) instead of DET have been reacted with ZS, which led to ZS-TET and ZS-TEP catalysts as presented in Scheme 2. FT-IR spectroscopy, TGA, SEM and TEM were used to characterize the obtained catalysts.
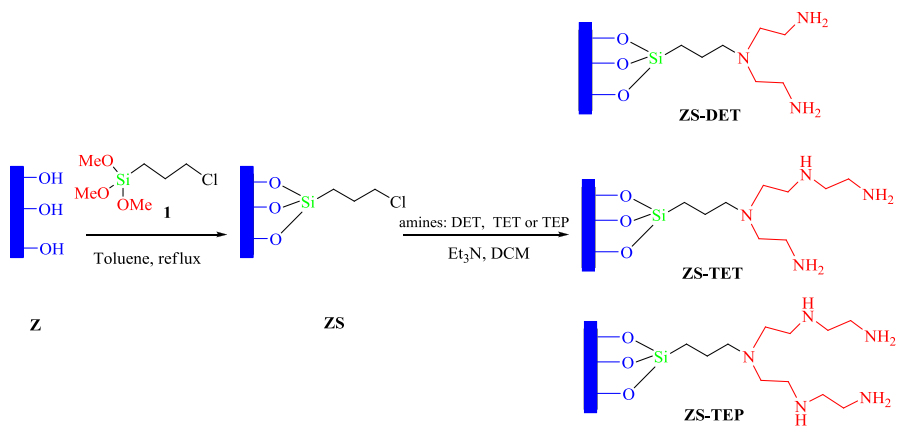
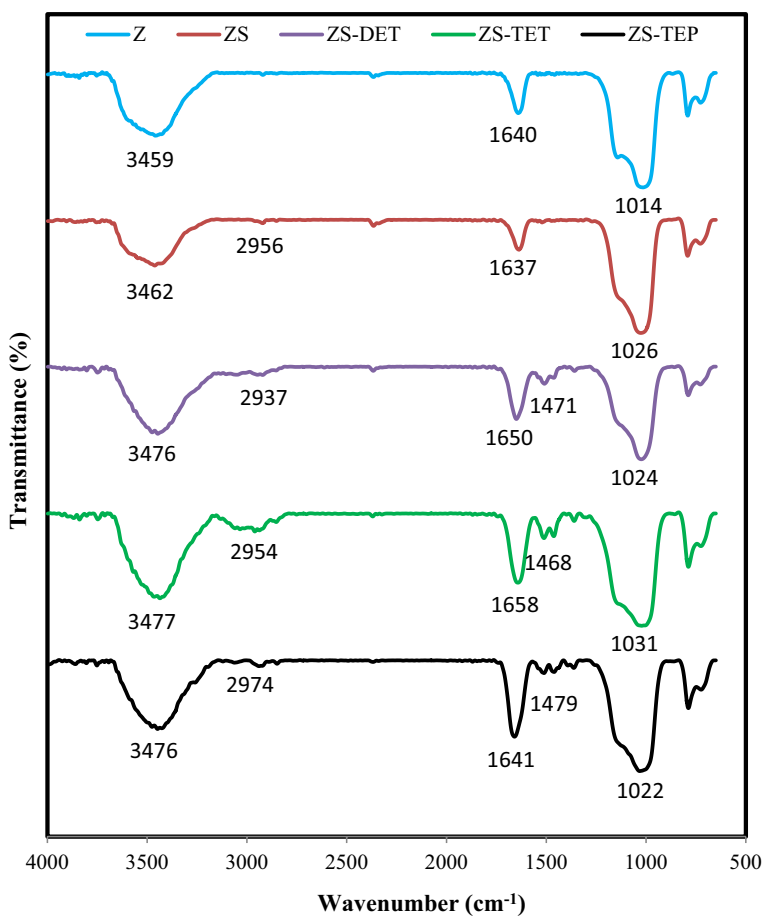**Scheme 2** Preparation of amine functionalized nanozeolites (ZS-DET, ZS-TET and ZS-TEP)

Fig. 1 IR spectra of Z, ZS, ZS-DET, ZS-TET and ZS-TEP

FT-IR spectra of Z, ZS, ZS-DET, ZS-TET and ZS-TEP are presented in Fig. 1. The IR spectrum of Z shows significant bands at 3473, 1640, and 1029 cm^{-1}, which are associated with O–H stretching vibrations corresponding to the hydrogen-bonded silanol groups, H–O–H bend and Si–O-Si asymmetric stretching vibrations, respectively [22]. The IR spectrum of ZS exhibits an additional absorption peak at 2800–2950 cm^{-1} relating to the C-H stretching of the $CH_2CH_2CH_2$–Cl group, confirming that CPTMS has been attached to the surface of Z. The IR spectrum of ZS-DET exhibits significant bands at 1640 and 1470 cm^{-1}, which can be related to NH_2 bending vibration for the primary amine group (RNH_2); a broad peak at 3473 cm^{-1} for N–H stretching vibration for the secondary amine group (R_2NH) [22–26]. The IR spectra of ZS-TET and ZS-TEP are as the same as that of ZS-DET. These outcomes prove that the ZS surface has been functionalized by TET and TEP, respectively.

Figures 2 and 3 show the TGA and DTA of the pure Z and modified ZSs with the diverse types of amines, respectively. The samples were heated from 30 °C to 600 °C by a speed of 10 °C per minute. The TGA profile of Z shows a weight loss occurred near 100 °C and a sharp weight loss appeared at 150 °C, which could be ascribed to the desorption of moisture or the surface absorbed water. The heating of pure Z from 160 to 600 °C, did not show any significant weight loss indicating the high thermal stability of zeolite. The ZS-DET, ZS-TET and ZS-TEP had two weight losses. The first weight loss region < 110 °C is because of the evaporation of the adsorbed water. The second region (for ZS-DET, ZS-TET and ZS-TEP 200–400 °C) can be mostly ascribed to the removal of aliphatic amine groups. Further, as it is clear the order of thermal stability based on char yield is: ZS-DET > ZS-TET > ZS-TEP.
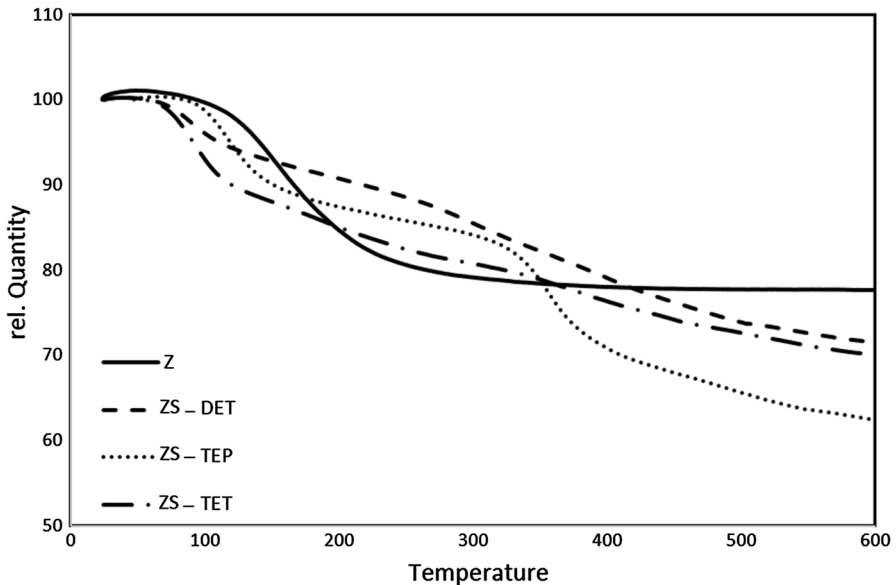

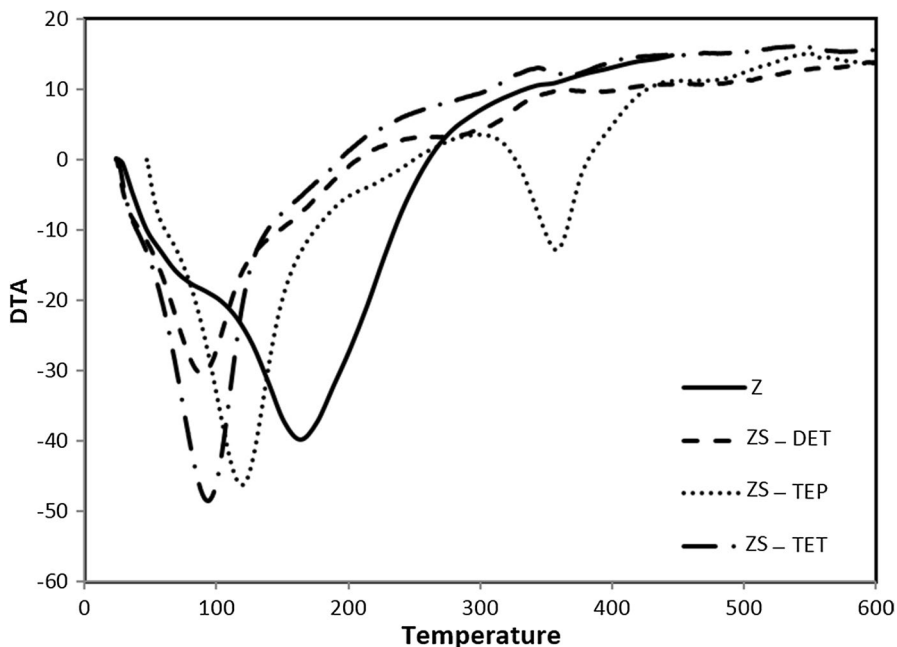**Fig. 2** TGA curves of pure Z, ZS and amine-modified ZSs

Fig. 3 DTA curves of pure Z, ZS and amine-modified ZSs

Table 1 CHN analysis of ZS and ZS-DET

Entry	Catalyst	C (wt%)	N (wt%)
1	ZS	4.17	–
2	ZS-DET	8.24	2.74

The amount of amine in the structure of ZS-DET was estimated to be about 1.84 mmol/g. In addition, the CHN analysis of ZS and ZS-DET is exhibited in Table 1. Increasing percent of carbon and nitrogen in ZS-DET clearly confirm the successful grafting of an amine group on the surface of ZS. According to the found N% from the CHN analysis, the amount of amine grafted onto ZS is nearly 1.30 mmol/g which is closed to the results obtained from TGA.

The morphology of the nanocatalysts surface was investigated by SEM as represented in Fig. 4. The uniform and flaky structure together with the existence of some particulates at the ZS-DET surface indicate that DET has been grafted to ZS. Particle size of Z, ZS and ZS-DET was provided by SEM with a mean size ranging from 16 to 23 nm as indicated in the related figure.

The TEM images of Z, ZS and ZS-DET are shown in Fig. 5 which show aggregated particles and do not give any information about the sample particle size.

The BET model of Z, ZS and ZS-DET is depicted in Fig. 6a, b. According to IUPAC classification, adsorption isotherms for Z and ZS are type I (Fig. 6a, b) while for ZS-DET it is type III (Fig. 6c). This data suggests that the structure of ZS-DET
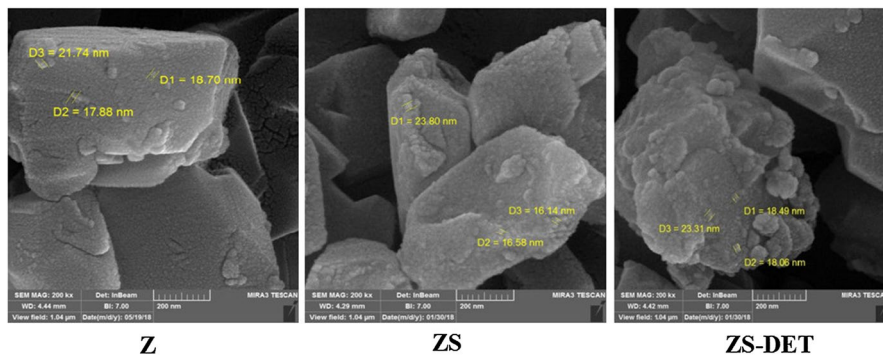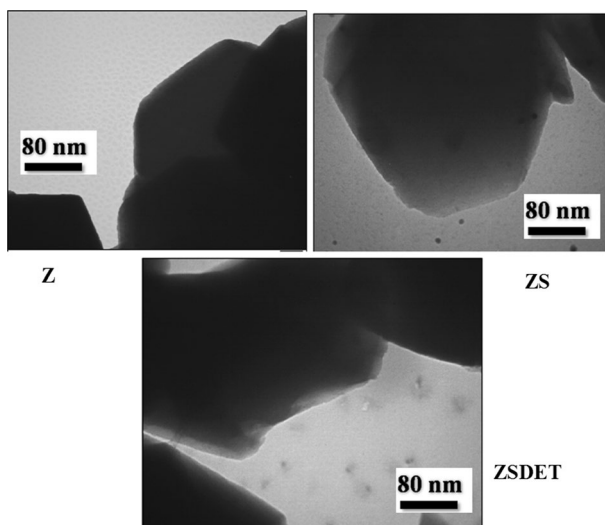
Fig. 4 SEM images of Z, ZS and ZS-DET

Fig. 5 TEM image of of Z, ZS and ZS-DET

has been changed from microporous to macroporous. The useful data was extracted from BET and t-plot curves of nanozeolites (Z, ZS and ZS-DET). As it can be seen from Table 2, total specific surface area (S_{BET}) reduced by functionalization of nanozeolite Z by silanated agent (ZS) followed by amination with DET (ZS-DET). This could be due to grafting of functional groups on the surface of Z and filling the pores thus reducing the surface area. This trend is also observed for total specific surface area (a_1), External specific surface area (a_2) and micropore area (a_1-a_2) which wasextracted from t-plot curves (Table 2). The result of the t-plot is not reported for the ZS-DET because of its macroporous structure.

Following our previous investigations on the improvement of green synthetic procedures for the preparation of heterocyclic compounds; herein, we report a
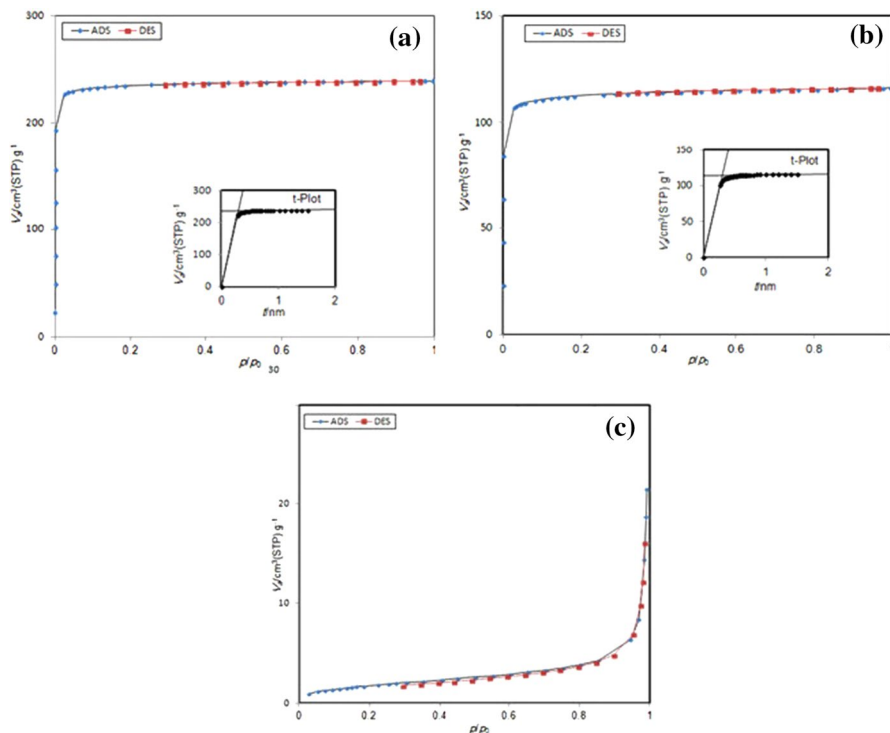
Fig. 6 BET plot and t-plot of Z (**a**), ZS (**b**) and ZS-DET (**c**)

Table 2 The pore structure properties of nanocatalysts that were calculated from BET model and t-plots

| Catalyst | BET | t-plot | | |
	Total specific surface area (S_{BET}, $m^2\,g^{-1}$)	Total specific surface area (a_1, $m^2\,g^{-1}$)	External specific surface area (a_2, $m^2\,g^{-1}$)	Micropore area ($a_1 - a_2$, $m^2\,g^{-1}$)
Z	934.0	1249.5	2.94	1246.55
ZS	452.7	572.8	1.93	570.91
ZS-DET	6.50	–	–	–

new green condition for synthesizing some pyrano[2,3-*c*]coumarins **4** from the condensation reaction of 4-hydroxycoumarin **1**, aromatic aldehydes **2** and malononitrile **3** in the presence of a catalytic amount of the synthesized modified nanozeolites (Scheme 3).

To achieve green reaction conditions, we examined a three-component reaction of malononitril, 4-bromo benzaldehyde and 4-hydroxycoumarin as a model reaction in the presence of a base nanonocatalyst (ZS-DET) in various solvents. As is observed in Table 3, EtOH is the optimal solvent in this reaction (entry 3).
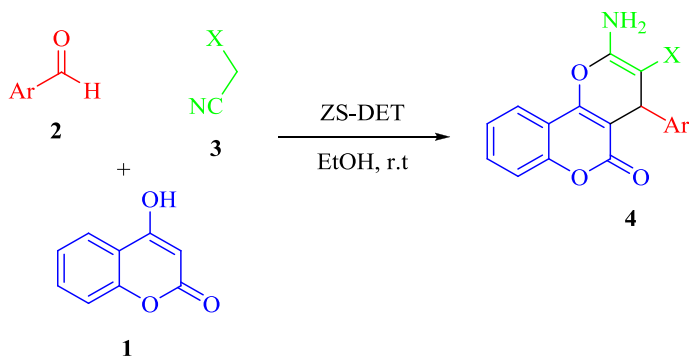
Scheme 3 Synthesis of pyrano[2,3-*c*]chromenes using ZS-DET

Table 3 Optimized condition of the reaction: 4-hydroxycoumarin (2 mmol), 4-bromo-benzaldehyde (2 mmol), and malononitrile (2 mmol), 10 mg catalyst in 10 mL solvent at ambient temperature

Entry	Catalyst	Solvent	Time (min)	Yield %[a]
1	ZS-DET	MeOH	60	65
2	ZS-DET	THF	60	trace
3	ZS-DET	EtOH	40	90
4	ZS-DET	EtOH:H_2O	60	trace
5	ZS-DET	H_2O	60	trace

[a]Isolated yields

Table 4 Optimized conditions for reactions of 4-hydroxycoumarin (2 mmol), 4-bromo-benzaldehyde (2 mmol), and malononitrile (2 mmol) in the existence of various amounts of ZS-DET as catalyst in EtOH at different times

Entry	ZS-DET (mg)	Time (min)	Yield %[a]
1	5	60	75
2	10	40	90
3	25	40	91
4	50	40	89
5	100	40	88

[a]Isolated yields

The reaction was performed using diverse amounts of ZS-DET as catalyst (5, 10, 25, 50 and 100 mg). The achieved outcomes in Table 4 show that ZS-TET is 10 mg at the optimized condition (Table 4, entry 2). Also, a higher amount of catalyst did not improve the results.

This reaction was studied in the presence of the prepared heterogeneous catalysts (Z, ZS, ZS-DET, ZS-TET and ZS-TEP). The obtained results in Table 5 well indicate that this reaction proceeds successfully in the presence of amine functionalized nanozeolites (ZS-DET, ZS-TET and ZS-TEP) while trace product obtained in the presence of Z or ZS (entries 3, 4 and 5 compared to entries 1 and 2). Among heterogeneous catalysts, ZS-DET was afforded to the product in the highest yield.

Table 5 Study of the reaction of 4-hydroxycoumarin (2 mmol), 4-bromo-benzaldehyde (2 mmol), and malononitrile (2 mmol) in the various catalysts

Entry	Catalyst	Amount of catalyst	Yield %[a]
1	Z	10 mg	Trace
2	ZS	10 mg	Trace
3	ZS-DET	10 mg	90
4	ZS-TET	10 mg	82
5	ZS-TEP	10 mg	76
6	DET	1 eq	98
7	DET	0.1 eq	95
8	TET	1 eq	90
9	TET	0.1 eq	85
10	TEP	1 eq	87
11	TEP	0.1 eq	82

[a]Isolated yields

Also, the reaction was tested with various equivalents of the homogenous catalysts (DET, TET and TEP) and then compared to the related heterogeneous catalysts. The outcomes show that when DET is used in the reaction, the highest yield is obtained (entries 6 and 7 compared to entries 8–11 in Table 5). Interestingly, the same trend is found for the desired heterogeneous catalysts (for example, entry 3 compared to entries 4 and 5 in Table 5). Considering the advantages of heterogeneous catalysts, such as easy separation and reusability, ZS-DET was selected as the optimal heterogeneous catalysts for this reaction.

Table 6 is provided to demonstrate the merit of this technique for synthesizing pyrano[2,3-c]coumarins in comparison with some previously reported ones [11, 27–32]. According to Table 6, DMAP was employed as a basic catalyst under refluxing EtOH. Although this method affords excellent yields, it suffers from the long time needed (entry 1). In the case of (S)-proline, the product is obtained in low yield with a long time (entry 2). Using some catalysts, such as diammonium

Table 6 Comparison of the literature outcomes for the preparation of **4b** with the results using this method

Entry	Catalyst/amount	Conditions	Time (min)	Yield (%) [Ref]
1	DMAP/20 mol%	EtOH/reflux	300	94 [27]
2	(S)-Proline/10 mol%	H_2O:EtOH/reflux	240	78 [11]
3	DAHP/10 mol%	H_2O:EtOH/r.t	180	85 [11]
4	Fe_3O_4/SiO_2-Met	H_2O:EtOH/reflux	260	86 [28]
5	Na_2WO_4 .$2H_2O$/5 mol%	H_2O:EtOH/r.t	150	82 [29]
6	Silica gel/300 wt%	EtOH/r.t	240	92 [30]
7	KF–Al_2O_3/0.125 g	EtOH/reflux	240	90 [31]
8	$H_6P_2W_{18}O_{62}$·$18H_2O$, 1 mol%	H_2O:EtOH/reflux	75	89 [32]
9	ZS-DET	EtOH/r.t	40	92[a]

[a]This work

hydrogen phosphate (DAHP) (entry 3), Fe_3O_4/SiO_2 -Met (entry 4), sodium tungstate (entry 5), Silica gel (entry 6), $KF–Al_2O_3$ (entry 7) and heteropoly acid (entry 8) results in a time-consuming reaction. We believe that these reactions can be efficiently carried out under our suggested conditions with respect to reaction times and product yield.

After optimization of the reaction conditions, to extend the scope of this reaction, a variety of aromatic aldehydes **2** were reacted with **1** and **3** (Table 7). Characterization of all the products was performed by comparing their spectra and physical data with those reported in the literature.

A mechanistic rationale is suggested for formation of pyranochromenes **4**, presented in Scheme 4. It appears that the reaction occurs in three phases. It is reasonable to assume that, the initial event involves the formation of the arylmethylene **5** via a Knoevenagel condensation of the aldehyde and malononitrile catalyzed by nano-ZS-DET. In the next steps, a Michael-type added to the arylmethylene and following heterocyclization stimulated by nano ZS-DET provides the relevant products **4**.

The key disadvantage of many developed approaches for these reactions is destruction of the catalysts in the workup process and so it cannot be retained or recycled. In these procedures, as shown in Fig. 7, the nano ZS-DET showed recyclability up to four cycles, for which there are insignificant losses in the catalytic performance. However, the SEM image of recycled ZS-DET, after recycling four times, was provided (Fig. 8) and compared with fresh catalyst (Fig. 4). Comparison of these two images showed no significant difference.

Table 7 Synthesis of 3,4-dihydropyrano[c]chromene derivatives

Product	Ar	X	Time (min)	Yield (%)[a]	Mp (°C)	Lit.Mp °C[Ref]
4a	4-Br–C_6H_4	CN	40	90	253–254	256–258 [11]
4b	4-Cl–C_6H_4	CN	30	92	260–261	262–264 [29]
4c	4-CN–C_6H_4	CN	30	94	291–293	289–290 [33]
4d	4-NO_2–C_6H_4	CN	45	90	257–259	258–260 [13]
4e	2-NO_2–C_6H_4	CN	60	88	256–257	252–255 [34]
4f	2,4-diCl–C_6H_3	CN	10	98	255–256	257–259 [11]
4g	3-OH–C_6H_4	CN	60	84	166–169	168–170 [34]
4h	4-Br–C_6H_4	CO_2Et	30	80	141–143	142–144 [27]
4i	4-Cl–C_6H_4	CO_2Et	30	84	195–196	192–194 [35]
4j	2,4-diCl–C_6H_3	CO_2Et	30	90	199–201	200–201 [36]
4k	4-CN–C_6H_4	CO_2Et	40	86	207–209	–
4l	4-NO_2–C_6H_4	CO_2Et	40	82	241–242	241–244 [27]
4m	2-NO_2–C_6H_4	CO_2Et	60	75	207–209	–

[a]Isolated yields
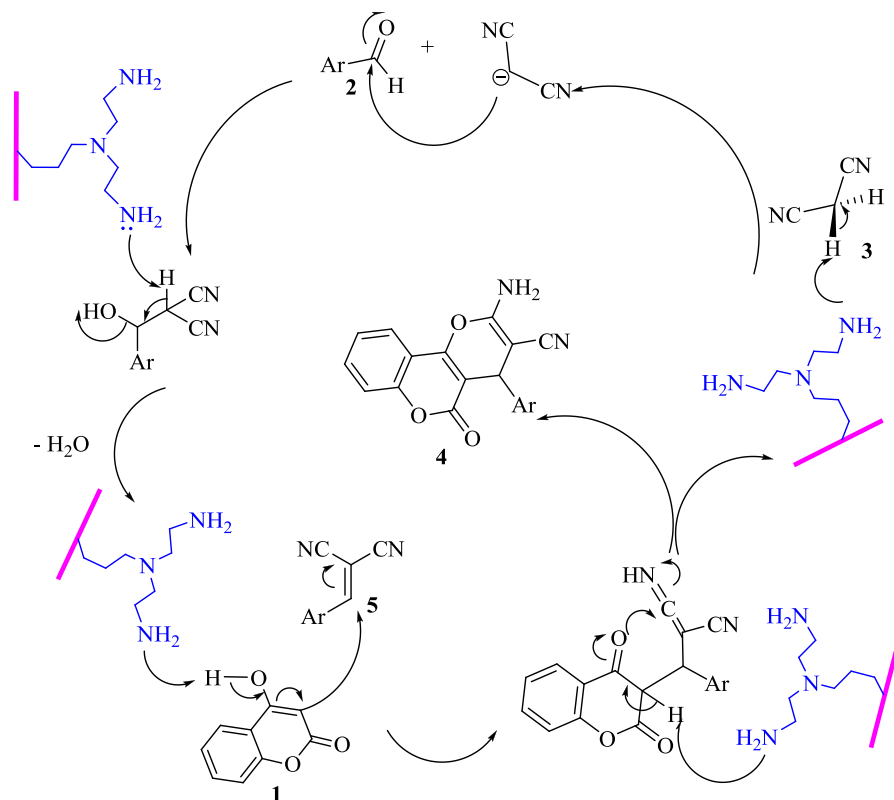
Scheme 4 The suggested mechanism for synthesizing pyranocoumarins **4** catalyzed by nano ZS-DET
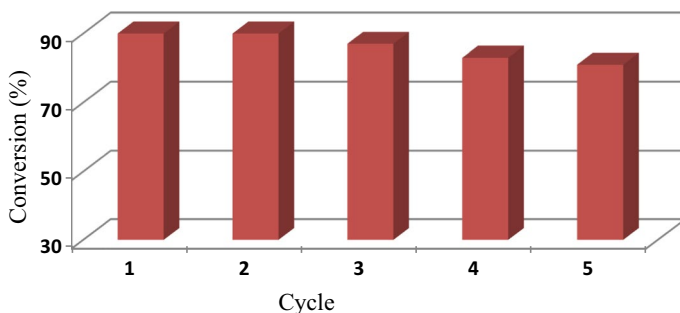

Fig. 7 Reusability of the catalysts in the model reaction (in 40 min)

Conclusions

In this study, initially, the silanated nanozeolite (ZS) was synthesized from the reaction of nanozeolite (Z) and CPTMS. Then, new modified nanozeolites (ZS-DET, ZS-TET and ZS-TEP) were synthesized from the reaction of ZS with
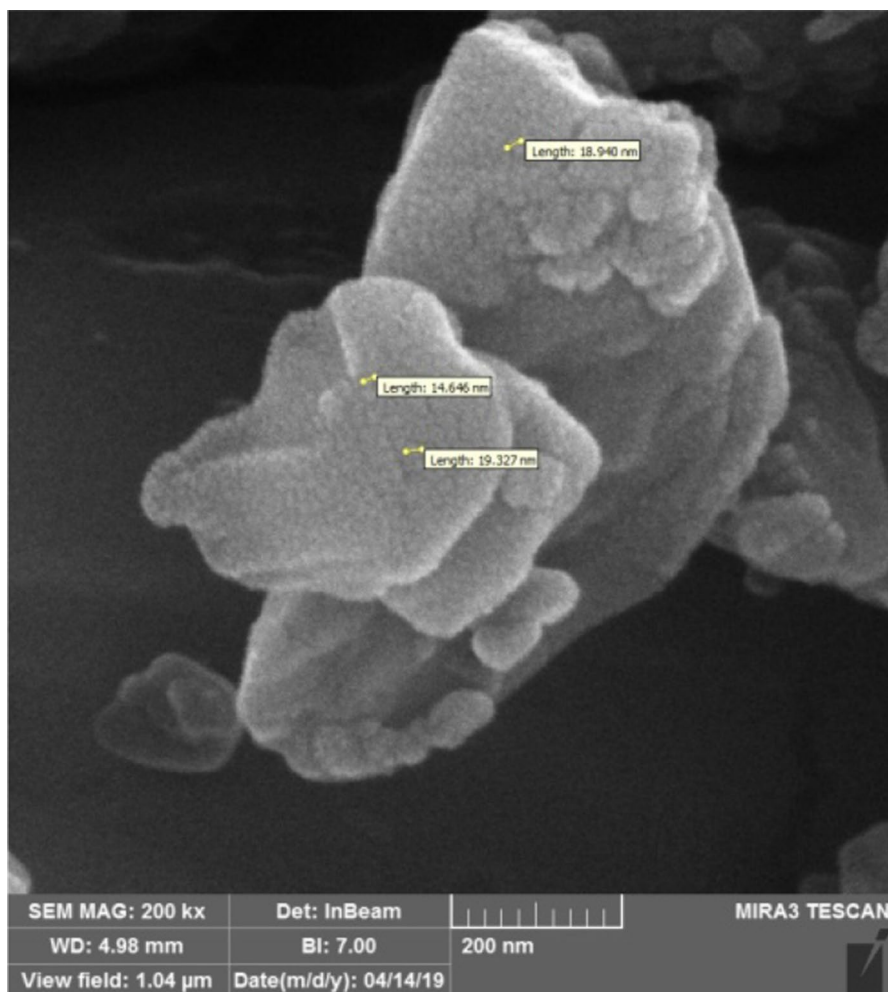
Fig. 8 SEM image of ZS-DET catalyst after recycling four times

multifunctional amines (DET, TET and TEP). FT-IR, TGA, DTG, SEM, and TEM were used to characterize the samples. Then, they were utilized in the reactions of aromatic aldehydes, malononitrile and 4-hydroxycoumarin as basic heterogeneous catalysts. Among the prepared catalysts, ZS-DET was a more effective catalyst to form pyrano[2,3-*c*]chromens than ZS-TET and ZS-TEP. Simple procedure, excellent efficiencies in short reaction times, inexpensive workup, ease of handling, cleaner reaction, and usage of reusable nanocatalyst are the attractive properties of this protocol.

References

1. D. Alexander, I. Ugi, Angew. Chem. Int. Ed. **39**, 3168 (2000)
2. D. Alexander, Chem. Rev. **106**, 17 (2006)
3. M. Syamala, Org. Prep. Proced. Int. **41**, 1 (2009)
4. E. Atsushi, A. Yanagisawa, M. Abe, Sh Tohma, T. Kan, T. Fukuyama, J. Am. Chem. Soc. **124**, 6552 (2002)
5. T. Lutz, A. Modi, Med. Res. Rev. **20**, 304 (2000)
6. C. Massimo, G. Cravotto, F. Epifano, G. Giannone, Curr. Med. Chem. **13**, 199 (2000)
7. Y.M. Litvinov, A.M. Shestopalov, Adv. Heterocycl. Chem. **103**, 175 (2011)
8. Ch. Lu, J. Lin, B. Chen, L. Zhao, Res. Chem. Intermed. **43**, 6691 (2017)
9. L. Bonsignore, G. Loy, D. Secci, A. Calignano, Eur. J. Med. Chem. **28**, 517 (1993)
10. C.S. Konkoy, D.B. Fick, S.X. Cai, N.C. Lan, J.F.W. Keana. PCT Int. Appl. WO 0075123, 2000. In Chem. Abstr (Vol. 134, p. 29313a, 2001)
11. A. Shahrzad, S. Balalaie, Tetrahedron Lett. **48**, 3299 (2007)
12. M.M. Heravi, B.A. Jani, F. Derikvand, F.F. Bamoharram, H.A. Oskooie, Catal. Commun. **10**, 272 (2008)
13. R.M. Shaker, Pharmazie **51**, 148 (1996)
14. J.M. Khurana, S. Kumar, Tetrahedron Lett. **50**, 4125 (2009)
15. A. Corma, H. Garcia, Catal. Today **38**, 257 (1997)
16. B.Z. Zhan, M.A. White, T.K. Sham, J.A. Pincock, R.J. Doucet, K.R. Rao, T.S. Cameron, J. Am. Chem. Soc. **125**, 2195 (2003)
17. W. Hölderich, M. Hesse, F. Näumann, Angew. Chem. Int. Ed. **27**, 226 (1988)
18. A. Corma, H. Garcia, Adv. Synth. Catal. **348**, 1391 (2006)
19. Zh Yahong, Y. Liu, J. Kong, P. Yang, Y. Tang, B. Liu, Small **2**, 1170 (2006)
20. L. Tosheva, V.P. Valtchev, Chem. Mater. **17**, 2494 (2005)
21. J. Liang, Z. Liang, R. Zou, Y. Zhao, Adv. Mater. **29**, 1701139 (2017)
22. X. Wang, V. Schwartz, J.C. Clark, X. Ma, S.H. Overbury, X. Xu, C. Song, J. Phys. Chem. C **113**, 7260 (2009)
23. F. Zheng, D.N. Tran, B.J. Busche, G.E. Fryxell, R.S. Addleman, T.S. Zemanian, C.L. Aardahl, Ind. Eng. Chem. Res. **44**, 3099 (2005)
24. A.C. Chang, S.S. Chuang, M. Gray, Y. Soong, Energy Fuels **17**, 468 (2003)
25. H.Y. Huang, R.T. Yang, D. Chinn, C.L. Munson, Ind. Eng. Chem. Res. **42**, 2427 (2003)
26. F. Su, C. Lu, S.C. Kuo, W. Zeng, Energy Fuels **24**, 1441 (2010)
27. A.T. Khan, M. Lal, S. Ali, M.M. Khan, Tetrahedron Lett. **52**, 5327 (2011)
28. A. Alizadeh, M.M. Khodaei, M. Beygzadeh, D. Kordestani, M. Feyzi, Bull. Korean Chem. Soc. **33**, 2546 (2012)
29. S. Khodabakhshi, M. Baghernejad, J. Chin. Chem. Soc. **61**, 521 (2014)
30. T.S.R. Prasanna, K.M. Raju, J. Korean Chem. Soc. **55**, 662 (2011)
31. X.S. Wang, Z.S. Zeng, D.Q. Shi, X.Y. Wei, Z.M. Zong, Chin. J. Org. Chem. **25**, 1138 (2005)
32. M.M. Heravi, B.A. Jani, F. Derikvand, F.F. Bamoharram, H.A. Catal, Commun. **10**, 272 (2008)
33. H.J. Wang, J. Lu, Z.H. Zhang, Monatsh. Chem. **141**, 1107 (2010)
34. D. Azarifar, M. Tadayoni, M. Ghaemi, Appl. Organomet. Chem. **32**, 4293 (2018)
35. H. Kiyani, M. Tazari, Res. Chem. Intermed. **43**, 6639 (2017)
36. D.Q. Shi, N. Wu, Q.Y. Zhuang, J. Chem. Res. **2008**, 542 (2008)

Affiliations

Fatemeh Babaei[1] · Sakineh Asghari[1,2] · Mahmoud Tajbakhsh[1]

✉ Sakineh Asghari
s.asghari@umz.ac.ir

[1] Department of Organic Chemistry, Faculty of Chemistry, University of Mazandaran, Babolsar 47416-95447, Iran

[2] Nano and Biotechnology Research Group, University of Mazandaran, Babolsar 47416-95447, Iran